Supplementary Material for

Fault Geometry Invariance for Physics-Informed Crustal Deformation Learning

Tomohisa Okazaki, Kazuro Hirahara, Naonori Ueda
RIKEN Center for Advanced Intelligence Project, Japan

Supplementary Text 1. The principle of fault geometry invariance is as follows: In Figure 2a, if $u_{\Sigma 1}(x,y)$ is the displacement field caused by a uniform slip s on Σ_1, the displacement field caused by the slip s on Σ_2 with the same dislocation lines is given by

$$u_{\Sigma 2}(x,y) = \begin{cases} u_{\Sigma 1}(x,y) + s & x \in D \\ u_{\Sigma 1}(x,y) & x \notin D \end{cases}, \tag{1}$$

where D is a domain enclosed by Σ_1 and Σ_2.

We verify this statement based on the governing equations. Assuming that $u_{\Sigma 1}(x,y)$ is a solution of the partial differential equation (PDE) system:

$$\mu \nabla^2 u_{\Sigma 1} + \nabla \mu \cdot \nabla u_{\Sigma 1} = 0 \ \text{ in } V, \tag{2}$$
$$u_{\Sigma 1}^{+} = u_{\Sigma 1}^{-} + s \ \text{ on } \Sigma_1, \tag{3}$$
$$\nabla_{\mathbf{n}^{\mathrm{DS}}} u_{\Sigma 1}^{+} = \nabla_{\mathbf{n}^{\mathrm{DS}}} u_{\Sigma 1}^{-} \ \text{ on } \Sigma_1, \tag{4}$$
$$\nabla_{\mathbf{n}^{\mathrm{FS}}} u_{\Sigma 1} = 0 \ \text{ on } S, \tag{5}$$

where $\mathbf{n}^{\mathrm{DS}}$ and $\mathbf{n}^{\mathrm{FS}}$ are the unit normal vectors, we show that $u_{\Sigma 2}(x,y)$ defined by Eq. (1) satisfies the same PDE system at different boundary locations:

$$\mu \nabla^2 u_{\Sigma 2} + \nabla \mu \cdot \nabla u_{\Sigma 2} = 0 \ \text{ in } V, \tag{6}$$
$$u_{\Sigma 2}^{+} = u_{\Sigma 2}^{-} + s \ \text{ on } \Sigma_2, \tag{7}$$
$$\nabla_{\mathbf{n}^{\mathrm{DS}}} u_{\Sigma 2}^{+} = \nabla_{\mathbf{n}^{\mathrm{DS}}} u_{\Sigma 2}^{-} \ \text{ on } \Sigma_2, \tag{8}$$
$$\nabla_{\mathbf{n}^{\mathrm{FS}}} u_{\Sigma 2} = 0 \ \text{ on } S. \tag{9}$$

Here, μ is the shear modulus and the superscripts $+$ and $-$ represent the right and left sides of Σ, respectively. Eqs. (2) and (6) represent the equilibrium equation of the elastic body, Eqs. (3) and (7) represent the displacement discontinuity on the fault, Eqs. (4) and (8) represent the traction continuity on the fault, and Eqs. (5) and (9) represent the free-surface conditions on the Earth's surface.

Eqs. (6) and (9) immediately follow from Eqs. (2) and (5), respectively, because $u_{\Sigma 1}$ and $u_{\Sigma 2}$ are different by a domain-wise constant, these equations only contain derivatives of u, and V and S are the same for the two fields. Therefore, we only have to inspect the consistency on Σ_1 and Σ_2, where the boundary location is different between the two fields. Because $u_{\Sigma 1}$ is smooth on Σ_2, the equalities $u_{\Sigma 1}^{+} = u_{\Sigma 1}^{-}$ and $\nabla_{\mathbf{n}^{\mathrm{DS}}} u_{\Sigma 1}^{+} = \nabla_{\mathbf{n}^{\mathrm{DS}}} u_{\Sigma 1}^{-}$ hold on Σ_2, which together with Eq. (1) yield Eqs. (7) and (8),respectively.

Finally, we must check that $u_{\Sigma 2}(x,y)$ is smooth across Σ_1, where $u_{\Sigma 1}(x,y)$ is discontinuous. Eqs. (1), (3) and (4) yield

$$u_{\Sigma 2}^{+} = u_{\Sigma 2}^{-} \ \text{ on } \Sigma_1, \tag{10}$$
$$\nabla_{\mathbf{n}^{\mathrm{DS}}} u_{\Sigma 2}^{+} = \nabla_{\mathbf{n}^{\mathrm{DS}}} u_{\Sigma 2}^{-} \ \text{ on } \Sigma_1. \tag{11}$$

Moreover, Eq. (3) with a constant s leads to

$$\nabla_{\mathbf{t}^{\mathrm{DS}}} u_{\Sigma 1}^{+} = \nabla_{\mathbf{t}^{\mathrm{DS}}} u_{\Sigma 1}^{-} \ \text{ on } \Sigma_1, \tag{12}$$

where $\mathbf{t}^{\mathrm{DS}}$ is the unit tangent vector, which together with Eq. (1) yields

$$\nabla_{\mathbf{t}^{\mathrm{DS}}} u_{\Sigma 2}^{+} = \nabla_{\mathbf{t}^{\mathrm{DS}}} u_{\Sigma 2}^{-} \ \text{ on } \Sigma_1. \tag{13}$$

Eqs. (11) and (13) yield

$$\nabla u_{\Sigma 2}^{+} = \nabla u_{\Sigma 2}^{-} \ \text{ on } \Sigma_1. \tag{14}$$

Eqs. (10) and (14) ensure that $u_{\Sigma 2}(x,y)$ is smooth on Σ_1. Therefore, $u_{\Sigma 2}(x,y)$ defined by Eq. (1) is a solution of the dislocation model caused by the uniform slip s on Σ_2.

The statement on Eq. (1) and its derivation provide key properties for antiplane crustal deformation.

Eqs. (4) and (12) give

$$\nabla u_{\Sigma 1}^{+} = \nabla u_{\Sigma 1}^{-} \ \text{ on } \ \Sigma_1, \tag{15}$$

which indicate that the strain field $\nabla u_{\Sigma 1}$ is continuous except the dislocation line. Additionally, Eq. (1) leads to $\nabla u_{\Sigma 1} = \nabla u_{\Sigma 2}$, that is, the two faults Σ_1 and Σ_2 produce the same strain field. Therefore, with respect to uniform slips, crustal deformation is essentially determined by the fault tip (dislocation line). In other words, the shape of the fault surface (dislocation surface) does not contribute to the strain field and can be regarded as a branch cut that alters the position of the displacement discontinuity.

Note that this does not hold true for distributed slips because Eq. (12) is replaced with

$$\nabla_{\mathbf{t}^{\mathrm{DS}}} u_{\Sigma 1}^{+} = \nabla_{\mathbf{t}^{\mathrm{DS}}} u_{\Sigma 1}^{-} + \nabla_{\mathbf{t}^{\mathrm{DS}}} s \ \text{ on } \ \Sigma_1, \tag{16}$$

which indicates that the strain field is discontinuous across the fault surface. Therefore, the shape of the dislocation surface contributes to the crustal deformation.

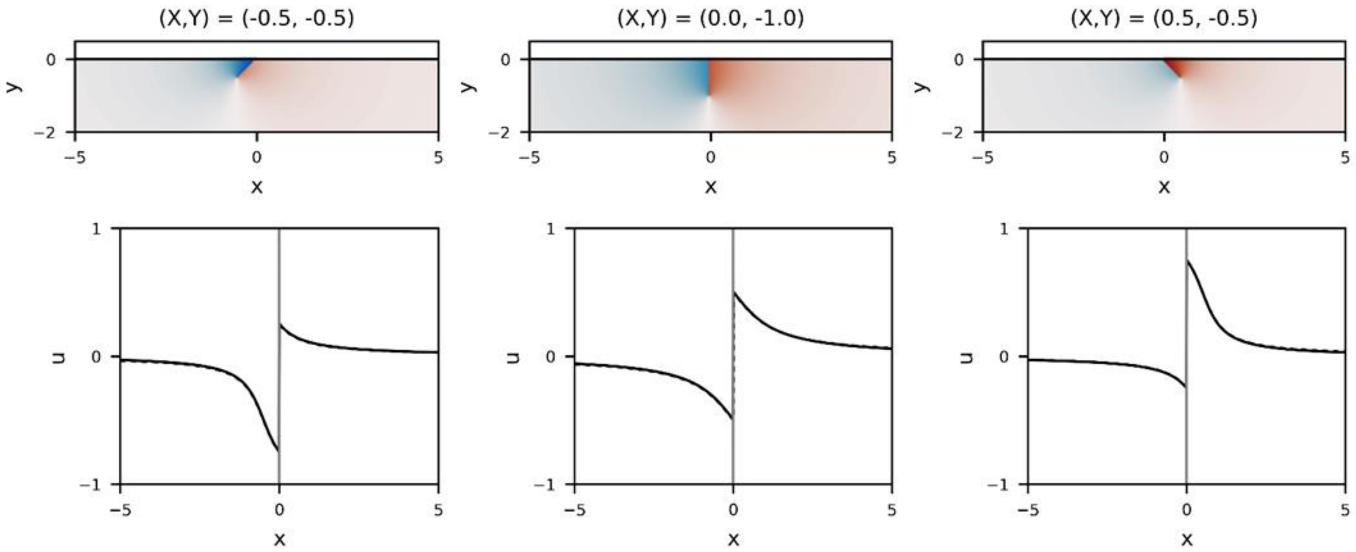

Supplementary Figure 1. The dislocation potential $\phi_{(X,Y)}(x, y)$ in the homogeneous half-space (Figure 4) learned by the physics-informed neural network. The Internal (top) and surface (bottom) displacements of selected (X, Y) are shown. In the top panels, the color scale is the same as that in Figure 1. In the bottom panels, dashed lines indicate analytical solutions.

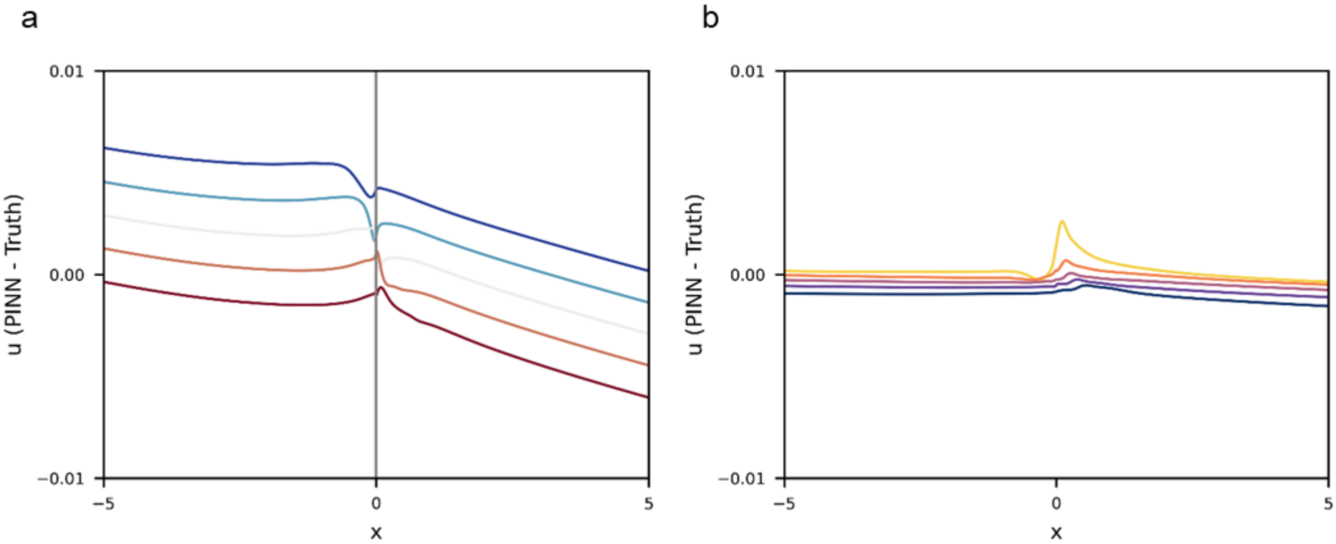

Supplementary Figure 2. Estimation errors of physics-informed neural networks in the homogeneous half-space. (a) Surface faults (Figure 4c). (b) Buried fault (Figure 4d).

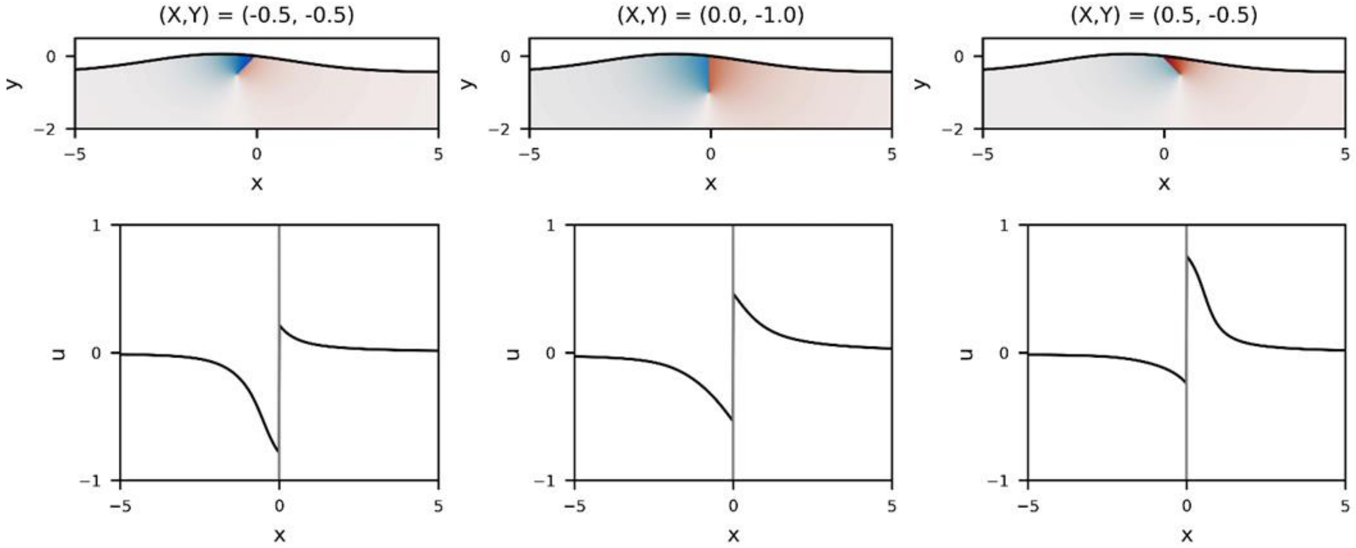

Supplementary Figure 3. The dislocation potential $\phi_{(X,Y)}(x, y)$ in the heterogeneous structure (Figure 5) learned by the physics-informed neural network. The internal deformation (top) and surface (bottom) displacements of selected (X, Y) are shown. In the top panels, the color scale is the same as that in Figure 1.

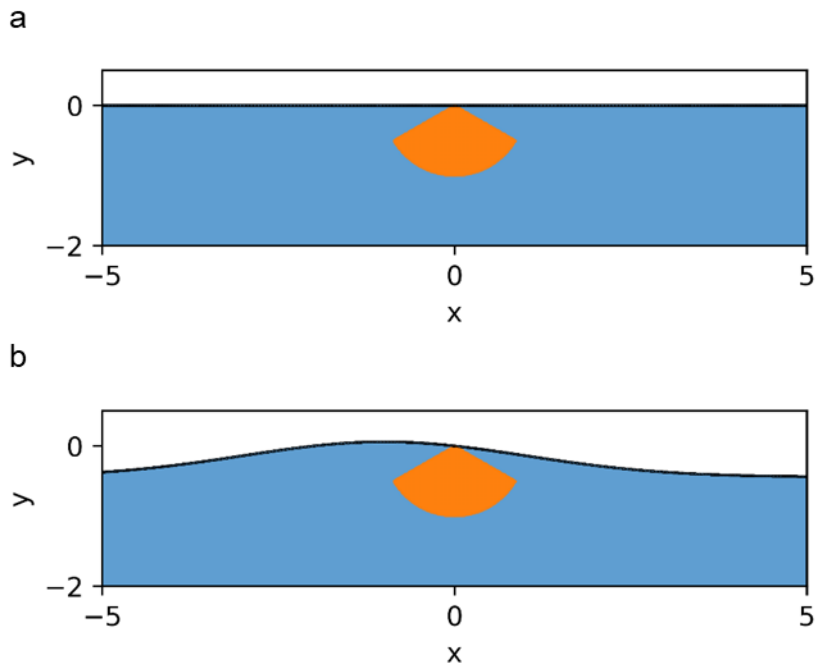

Supplementary Figure 4. Range of collocation points in training of physics-informed neural networks. (a) Homogeneous half-space (Figure 4). (b) Heterogeneous structure (Figure 5). Blue and orange regions represent the ranges of spatial coordinates (x, y) and dislocation lines (X, Y), respectively. Black lines indicate ground surfaces.

Supplementary Table 1. The root-mean-square errors of the physics-informed neural network estimation for the variable faults in the half-space (Figure 4a, c).

Peak position x	Absolute error	Norm	Relative error
-0.6	0.004263	0.1863	0.0229
-0.3	0.002877	0.1615	0.0178
0	0.001897	0.1505	0.0126
0.3	0.001971	0.1615	0.0122
0.6	0.003022	0.1863	0.0162

Supplementary Table 2. The root-mean-square errors of the physics-informed neural network estimation for the variable slips in the half-space (Figure 4b, d).

Peak position y	Absolute error	Norm	Relative error
-0.3	0.000507	0.0173	0.0293
-0.4	0.000240	0.0164	0.0146
-0.5	0.000423	0.0167	0.0253
-0.6	0.000710	0.0176	0.0403
-0.7	0.001053	0.0187	0.0563

Supplementary Table 3. Number of collocation points in the L-BFGS optimizer.

Structure	Domain (V)	Fault surface (Σ)	Ground surface (*S*)
Homogeneous (Figure 4)	212100	5810	21105
Heterogeneous (Figure 5)	196035	5810	21105